Chinese Chemical Letters 33 (2022) 2569–2572

Contents lists available at ScienceDirect

Chinese Chemical Letters

journal homepage: www.elsevier.com/locate/cclet

Quasi-continuous synthesis of cobalt single atom catalysts for transfer hydrogenation of quinoline

Liyun Huang[a,d,1], Hao Zhang[a,1], Yujie Cheng[a], Qingdi Sun[a], Tao Gan[a], Qian He[a,*], Xiaohui He[a,b], Hongbing Ji[a,b,c,*]

[a] Fine Chemical Industry Research Institute, School of Chemistry, Sun Yat-sen University, Guangzhou 510275, China
[b] Huizhou Research Institute of Sun Yat-sen University, Huizhou 516216, China
[c] School of Chemical Engineering, Guangdong University of Petrochemical Technology, Maoming 525000, China
[d] School of Environmental and Chemical Engineering, Foshan University, Foshan 528000, China

ARTICLE INFO

Article history:
Received 31 July 2021
Revised 19 September 2021
Accepted 4 October 2021
Available online 8 October 2021

Keywords:
Quasi-continuous synthesis
Single atom catalysts
Microcapsule
Transfer hydrogenation
Quinoline

ABSTRACT

Improving the transfer hydrogenation of *N*-heteroarenes is of key importance for various industrial processes and remains a challenge so far. We reported here a microcapsule-pyrolysis strategy to quasi-continuous synthesis S, N co-doped carbon supported Co single atom catalysts (Co/SNC), which was used for transfer hydrogenation of quinoline with formic acid as the hydrogen donor. Given the unique geometric and electronic properties of the Co single atoms, the excellent catalytic activity, selectivity and stability were observed. Benefiting from the quasi-continuous synthesis method, the as-obtained catalysts provide a reference for the large-scale preparation of single atom catalysts without amplification effect. Highly catalytic performances and quasi-continuous preparation process, demonstrating a new and promising approach to rational design of atomically dispersed catalysts with maximum atomic efficiency in industrial.

Transfer hydrogenation of *N*-heteroarenes is an essential process for synthesizing important intermediates applied in the pharmaceutical, agrochemical and petrochemical fields [1,2]. In this process, formic acid, as a "liquid hydrogen donor", has received wildly interest for catalytic transfer hydrogenation [3], and the selective hydrogenation of *N*-heteroarenes has become one of the most challenging reactions due to their high resonance stability and the possible poisoning of the catalyst [3]. So far, much work of transfer hydrogenation reactions has focused on the precious metals-based heterogeneous catalysts, *e.g.*, Pt [4,5], Pd [6], Rh [7,8], Au [9,10] and Ru [11,12]. However, the high cost and rareness of such noble metal catalysts restrict their practical applications. From the viewpoint of economic and environmental perspectives, developing a low-cost and earth-abundant metal catalyst with satisfactory activity, selectivity and stability for realizing the efficient transformations of various *N*-heterocycles is highly desirable.

In recent years, nitrogen-doped porous carbon loading transition metal nanoparticles (NPs), such as Fe, Co [3,13,14], have been considered to be one of the most cost-effective heterogeneous catalysts for selective hydrogenation of *N*-heterocycles. Yun *et al.* [14] recently reported a nitrogen (N)-doped carbon nanotube encapsulated Co NPs to achieve a high catalytic activity in selective hydrogenation of quinolines. Chen *et al.* [3] prepared a Co NPs anchored on N-doped carbon (Co/Melamine-2@C-700), which displayed high activity and selectivity for the reduction of diverse *N*-heteroarenes. Despite these achievements, because heterogeneous catalysis usually occurs on the surface of the catalysts, to further enhance the catalytic properties, it is necessary to downsize the metal NPs to obtain more exposed active sites.

Single-atom catalysts (SACs) [15], theoretical 100% atom utilization efficiency and superior catalytic properties [16–19], have emerged as a rising star used as ideal models to deeply understand the mechanism of the reaction at the atomic level. In particular, due to the great advantages in huge surface area and strong thermal stability [20], N-doped carbon-supported atomically dis-

* Corresponding authors at: Fine Chemical Industry Research Institute, School of Chemistry, Sun Yat-sen University, Guangzhou 510275, China.
E-mail addresses: heqian27@mail.sysu.edu.cn (Q. He), jihb@mail.sysu.edu.cn (H. Ji).
[1] These authors contributed equally to this work.

https://doi.org/10.1016/j.cclet.2021.10.004
1001-8417/

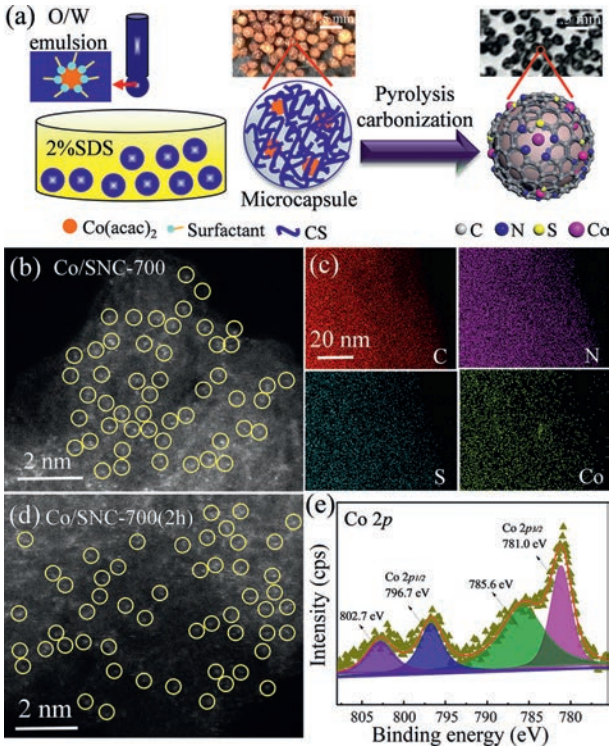

Fig. 1. (a) Scheme of the *quasi*-continuous synthesis of Co/SNC. (b) AC HAADF-STEM of Co/SNC. (c) EDS elemental mapping of Co/SNC. (d) AC HAADF-STEM of Co/SNC(2h) catalysts. (e) XPS of Co/SNC.

persed transition metal (M-N-C, M = Fe, Co, Ni, Cu, *etc.*) exhibit superior catalytic performance in various reactions, *e.g.*, oxygen reduction reaction [21,22], CO oxidation [23], CO_2 reduction [24,25], *etc*. Besides, it is found that co-doping S atoms in M-N-C single-site catalysts (M/SNC) could further improve the catalytic performance in electrochemical reactions and organic reactions, mainly because S atom possesses a weaker electronegativity and bigger in size than N it is expected that partially displacing the N electronic band structure in the MN_4 structure with S atoms can significantly influence the ΔG_{H^*} value of the transition metal [26–28]. Although progress has been made on the synthesis of M/SNC SACs, most of these strategies are batch-type, which seriously hinder the mass production and practical application of SACs due to the discontinuity, low efficiency and poor batch-to-batch reproducibility. It is therefore highly desirable to develop a facile method for continuous production of S, N co-doped carbon-supported SACs.

Here, we adopt the microencapsulation-pyrolysis strategy for quasi-continuous synthesis of S, N co-doped carbon catalyst with a single Co atom site (Co/SNC) without acid leaching to remove metal nanoparticles [29–31]. The synthesized Co/SNC can realize highly efficient selective hydrogenation of quinoline and its derivatives into corresponding 3,4-dihydroquinoline-1(2*H*)-carbaldehyde. The reported approach offers an alternative way for the continuous synthesis of various transitional metal SACs.

The Co/SNC catalyst was synthesized as Fig. 1a. In brief, the $Co(acac)_2$ as metal precursors were encapsulated in chitosan/sodium dodecyl sulfate (CS/SDS) hydrogel, and a large number of C, N and S atoms would be introduced at the same time. The continuous preparation of $Co(acac)_2$ microcapsules through a droplet-generating device can achieve a yield of about 180 mL/h (~1 g catalyst after pyrolysis). Then, the prepared microcapsules were pyrolysis at 700 °C under a nitrogen atmosphere to obtain Co/SNC catalysts. The content of Co atoms in the Co/SNC catalyst was approximately 0.85 wt% determined by inductively coupled plasma optical emission spectrometry (ICP-OES) analysis (Table S1 in Supporting information). Transmission electron microscopy (TEM) and dark-field scanning transmission electron microscopy (STEM) images of Co/SNC catalyst (Figs. S1a and b in Supporting information) showed that no Co nanoparticles were observed. In addition, as seen from the image taken by aberration-corrected high-angle annular dark-field scanning transmission electron microscopy (AC HAADF-STEM) (Fig. 1b), Co single atoms were circled in yellow as isolated bright dots. Furthermore, elemental mapping spectroscopy demonstrated that all the elements of Co, N, S and C were uniformly distributed (Fig. 1c), indicating the Co single atoms were dispersed uniformly on S, N co-doped carbon. More interestingly, when our catalyst fabrication time was selected at the second hour, for Co/SNC(2h) in Fig. 1d, the Co species were also atomically dispersed on the carbon supports (marked by the yellow circles) without distinct Co aggregations, demonstrating the good control quality in our approach. The X-ray diffraction (XRD) pattern of Co/SNC exhibited two diffraction peaks at 24.7° and 44.0°, C(002) and a C(100) [32], respectively, indicating the graphitic carbon nature of our catalyst (Fig. S2 in Supporting information). The Brunauer-Emmett-Teller (BET) surface area of Co/SNC was 125 m^2/g, and the high specific surface area promotes the chemical reaction and mass transfer [33]. The X-ray photoelectron spectroscopy (XPS) survey revealed that the Co/SNC mainly consisted of Co, N, S, C and O elements (Fig. 1e and Fig. S3 in Supporting information). There were two main peaks located at about 781.0 eV and 796.7 eV in high resolution of Co 2p spectra (Fig. 1e), which can be assigned to Co $2p_{3/2}$ and Co $2p_{1/2}$ [32], respectively, indicating the mixed-valence of Co^{2+} and Co^{3+}. High-resolution N 1s peak showed four main peaks corresponding to the pyrrolic N (398.4 eV), pyridinic N (399.8 eV), graphitic N (400.8 eV), and oxidized N (406.6 eV) (Fig. S3b) [34]. The high-resolution S 2p peak showed two main peaks attributed to C-S-C at 165.2 and 164.0 eV and one peak assigned to $-SO_x$ (Fig. S3c) [35].

The X-ray absorption fine structure (XAFS) measurements were conducted to investigate the chemical state and local coordination structure of the Co atoms in Co/SNC. The Co K-edge X-ray absorption near edge structure (XANES) spectra of Co/SNC, Co foil, Co_3O_4 and CoO were shown in Fig. 2a. The absorption edges indicated that the valence of Co atoms in Co/SNC was between Co^0 and Co^{3+} [36], which was in line with the XPS results. As shown in Fig. 2b, the Co/SNC displayed a strong peak near 1.4 Å and a weak peak near 1.6 Å, corresponding to Co−N bonding and Co−S bonding [37,38], respectively, and no obvious Co−Co peak (2.2 Å) was detected [37]. Moreover, compared with the contour map of Co foil reference in wavelet transforms (WT, Fig. 2c), it is found that the intensity maximum of Co−Co coordination (7.5 $Å^{-1}$) was not observed in Co/NSC (3.9 $Å^{-1}$), which confirmed that the Co species in Co/SNC were strictly isolated [39]. According to the extended X-ray absorption fine structure spectrometry (EXAFS) fitting results, the coordination number of the Co atoms with surrounding N atoms and S atoms were 3.4 ± 0.7 and 0.7 ± 0.1, respectively, manifesting that the single Co atom was coordinated with three N atoms and one S atom (CoN_3S-like structure, Fig. 2d and Table S2 in Supporting information) [40].

The as-obtained catalysts were examined the catalytic activity for transfer hydrogenation of quinoline with formic acid as a hydrogen source to 3,4-dihydroquinoline-1(2*H*)-carbaldehyde (Fig. 3). The conversion-time profile of Co/SNC catalysts was shown in Fig. 3a. Results showed that the Co/SNC catalyst could display excellent reaction performance (98% conversion and 99% selectivity) after reaction for 4 h. Under the same reaction conditions, the conversions over Co/NC, Co-NPs (11.2 nm in diameter shown in Fig. S4 in Supporting information; same cobalt loading as Co/SNC), metal-free SNC catalyst, $Co(acac)_2$ and blank experiment were only 56%, 50%, 13%, 9% and 10%, respectively, demonstrating that the Co sin-

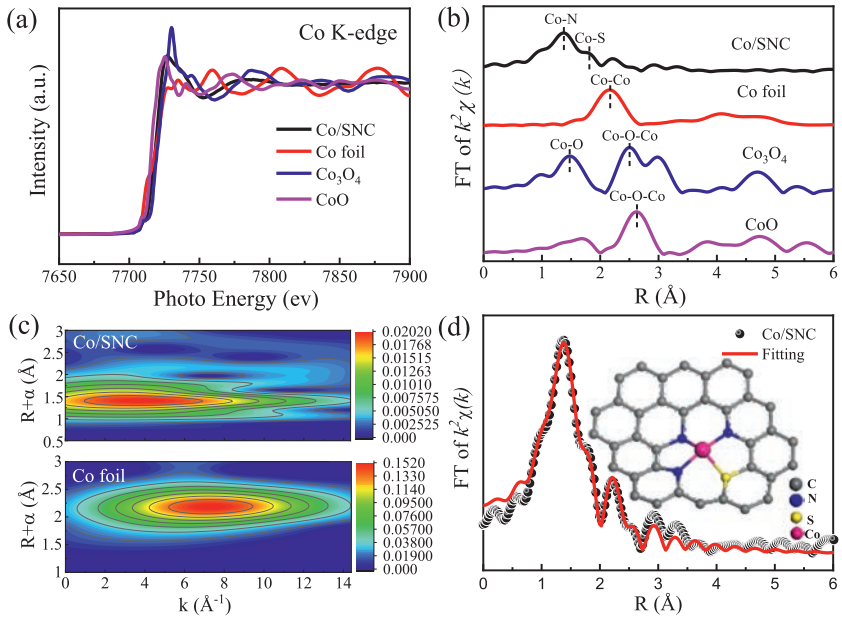

Fig. 2. (a) Normalized XANES of Co/SNC, Co foil, Co_3O_4, CoO. (b) Magnitudes of Fourier-transforms (FT) spectra of EXAFS for Co/SNC, Co foil, Co_3O_4, CoO. (c) The wavelet transforms (WT) for the k^{3-} weighted EXAFS signals. (d) The corresponding EXAFS R space fitting curves of Co/SNC, inset displays the model of Co/SNC.

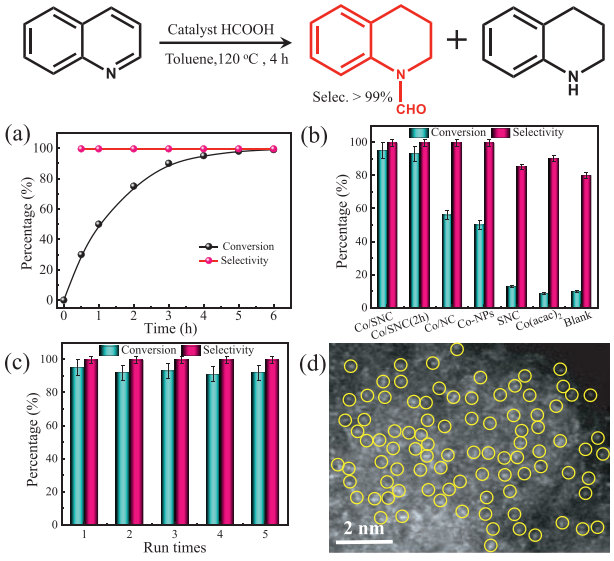

Fig. 3. Performance evaluation for transfer hydrogenation of quinoline. (a) The quinoline hydrogenation performance of the Co/SNC catalyst at different reaction times. (b) Catalytic activity for transfer hydrogenation of quinolines with formic acid as a hydrogen source by Co/SNC, Co/SNC(2h), Co/NC, Co-NPs, SNC, $Co(acac)_2$ and blank condition. (c) Recycle reaction results of Co/SNC catalysts. (d) AC HAADF-STEM image of the used Co/SNC catalysts. Reaction conditions: C_0 (quinoline) = 0.25 mmol, catalyst dosage = 30 mg, toluene = 1.5 mL, C_0 (formic acid) = 5 mmol, T = 120 °C, reaction time = 4 h.

gle atoms in Co/SNC catalysts play a key role in promoting the transfer hydrogenation of quinoline (Fig. 3b). To our great delight, the catalysts of Co/SNC and Co/SNC(2h) exhibited almost the same catalysis properties (~95% conversion and ~99% selectivity), indicating the two Co/SNC catalysts possessed identical catalytically active sites in the transfer hydrogenation of quinoline. More importantly, the Co/SNC still maintained high reactivity (92% conversion and 99% selectivity) after five runs (Fig. 3c), without any obvious metal loss (0.85 wt% *vs.* 0.83 wt%) or observed metal aggregation (Fig. 3d). These results indicated the good structural stability and reusability of our Co/SNC catalyst possessed, which was significantly important in industry applications. Next, the formic acid dehydrogenation over the Co/SNC catalyst was performed at 120 °C without any additives (Fig. S5 in Supporting information). It was found that the Co/NC, Co-NPs, metal-free SNC catalyst, $Co(acac)_2$ and blank experiments exhibited a low gas-production rate (GPR, < 50 mL g^{-1} h^{-1}) in formic acid dehydrogenation. As expected, the catalytic activity was significantly increased when using Co/SNC as the catalysts (GPR = 175 mL g^{-1} h^{-1}), which can be ascribed to the highly dispersed Co species. Thus, these Co/SNC catalysts were also of significant interest for hydrogen generation processes.

Co/SNC was further tested for transfer hydrogenation of a variety of *N*-heterocyclic substrates. As shown in Table 1, an electron-donating group in quinoline derivatives (–Me or –OMe), transfers hydrogenation up to 90% conversion and 99% selectivity (Table 1, entries 1 and 2). As expected, an electron-withdrawing group in quinoline derivatives (–COOMe, –F, –Ph) were also converted to the desired products in high to excellent conversions (Table 1, entries 3–5). Moreover, a 90% conversion of 7-fluoro-2-methyl-quinoline into 7-fluoro-2-methyl-3,4-dihydroquinoline-1(2*H*)-carbaldehyde was observed (Table 1, entry 6). Apart from quinoline derivatives, *N*-heteroarenes such as phthalazine, superior conversion and high selectivity were also achieved (Table 1, entry 7).

In summary, we have developed a *quasi*-continuously synthesized of atomically dispersed Co/SNC catalysts through the microcapsule pyrolysis strategy. The synthesized Co/SNC exhibits remarkable activity, selectivity and reusability for transfer hydrogenation of quinoline with formic acid as a hydrogen source (up to 95% conversions and 99% selectivity). In addition, a broad range of *N*-heterocyclic substrates including quinoline derivatives and phthalazine were realized with the Co/SNC catalysts. More inspiringly, our microcapsule precursor method endowed Co SACs catalysts obtained from different time [Co/SNC and Co/SNC(2 h)] with very similar catalytic sites, evidenced by structural characterization and catalytic-performance evaluation results. In brief, this work provides a simple strategy for the quasi-continuous production of cat-

Table 1
Transfer hydrogenation of quinolines with formic acid catalyzed by Co/SNC[a].

Entry	Substrate	Product	Conv. (%)	Selec. (%)
1			99	99
2	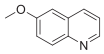	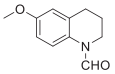	95	99
3	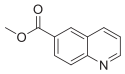	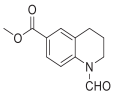	94	99
4			80	99
5	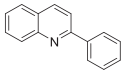	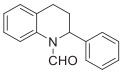	85	99
6	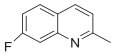	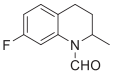	90	99
7		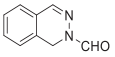	99	99

[a] Reaction conditions: substrate (0.1 mmol), catalyst (30 mg), formic acid (5 mmol), toluene (1.5 mL), 120 °C, 12 h. The conversions and gas chromatography (GC) yields were calculated by using of *n*-dodecane as an internal standard. The molecular structures of products were characterized by NMR and mass spectrum (Figs. S5-S20 in Supporting information).

alysts with atomically dispersed Co sites for transfer hydrogenation reactions, conducive to catalytic research and industrial production.

Declaration of competing interest

The authors report no declarations of interest.

Acknowledgments

We acknowledge the financial support from the National Natural Science Foundation of China (Nos. 22078371, 21938001, 21961160741), Guangdong Provincial Key R&D Programme (No. 2019B110206002), Special fund for Local Science and Technology Development by the Central Government, Local Innovative and Research Teams Project of Guangdong Pearl River Talents Program (No. 2017BT01C102), the NSF of Guang-dong Province (No. 2020A1515011141), the National key Research and Development Program Nanotechnology Specific Project (No. 2020YFA0210900), the Science and Technology Key Project of Guangdong Province, China (No. 2020B010188002), The Project Supported by Guangdong Natural Science Foundation (No. 2021A1515010163).

Supplementary materials

Supplementary material associated with this article can be found, in the online version, at doi:10.1016/j.cclet.2021.10.004.

References

[1] M. Tang, J. Deng, M. Li, et al., Green Chem. 18 (2016) 6082–6090.
[2] M. Pang, J.Y. Chen, S. Zhang, et al., Nat. Commun. 11 (2020) 1249.
[3] F. Chen, B. Sahoo, C. Kreyenschulte, et al., Chem. Sci. 8 (2017) 6239–6246.
[4] S. Li, Y. Yang, Y. Wang, et al., Catal. Sci. Technol. 8 (2018) 4314–4317.
[5] N. Zhang, Q. Shao, X. Xiao, X. Huang, Adv. Funct. Mater. 29 (2019) 1808161.
[6] M. Guo, C. Li, Q. Yang, Catal. Sci. Technol. 7 (2017) 2221–2227.
[7] A. Karakulina, A. Gopakumar, I. Akcok, et al., Angew. Chem. Int. Ed. 55 (2016) 292–296.
[8] M. Nasiruzzaman Shaikh, M.A. Aziz, A.N. Kalanthoden, et al., Catal. Sci. Technol. 8 (2018) 4709–4717.
[9] D. Ren, L. He, L. Yu, et al., J. Am. Chem. Soc. 134 (2012) 17592–17598.
[10] J. Zhao, Q. Li, S. Zhuang, et al., J. Phys. Chem. Lett. 9 (2018) 7173–7179.
[11] D. He, X. Xu, Y. Lu, M.J. Zhou, X. Xing, Org. Lett. 22 (2020) 8458–8463.
[12] M. Fang, R.A. Sánchez-Delgado, J. Catal. 311 (2018) 357–368.
[13] Z. Wei, Y. Chen, J. Wang, et al., ACS Catal. 6 (2016) 5816–5822.
[14] R. Yun, L. Hong, W. Ma, et al., ChemCatChem 12 (2020) 129–134.
[15] J. Zhang, C. Liu, B. Zhang, Small Methods 3 (2019) 1800481.
[16] S. Ji, Y. Chen, X. Wang, et al., Chem. Rev. 120 (2020) 11900–11955.
[17] H. Zhang, Y. Liu, T. Chen, J. Zhang, X.W. Lou, Adv. Mater. (2019) 1904548.
[18] X. Wu, H. Zhang, S. Zuo, et al., Nanomicro Lett. 13 (2021) 136.
[19] H. Zhang, Y. Wang, S. Zuo, et al., J. Am. Chem. Soc. 143 (2021) 2173–2177.
[20] L. Zhao, Y. Zhang, L. Huang, et al., Nat. Commun. 10 (2019) 1278.
[21] A. Han, W. Chen, S. Zhang, et al., Adv. Mater. 30 (2018) 1706508.
[22] P. Yin, T. Yao, Y. Wu, et al., Angew. Chem. Int. Ed. 55 (2016) 10800–10805.
[23] C. Jia, X. Wang, H. Yin, et al., J. Mater. Chem. A 9 (2021) 2093–2098.
[24] K. Jiang, S. Siahrostami, T. Zheng, et al., Energ. Environ. Sci. 11 (2018) 893–903.
[25] G. Xu, H. Zhang, W. Jing, H.X. Zhang, J. Ye, ACS Nano 12 (2018) 5333–5340.
[26] J. Zhang, M. Zhang, Y. Zeng, et al., Small 15 (2019) 1900307.
[27] Y. Wang, S. Zhang, X. Meng, et al., ACS Appl. Mater. Inter. 13 (2021) 503–513.
[28] J. Wang, Q. Wang, W. She, et al., J. Power Sources 418 (2019) 50–60.
[29] R.Q. Zhong, C.X. Zhi, Y.X. Wu, et al., Chin. Chem. Lett. 31 (2020) 1588–1592.
[30] W.K. Wang, S.B. Zhang, Y.Y. Liu, et al., Chin. Chem. Lett. 32 (2021) 805–810.
[31] A.Q. Xiang, S. Xie, F. Pan, et al., Chin. Chem. Lett. 32 (2021) 830–833.
[32] H. Shi, Y. Li, P. Lu, Z.S. Wu, Acta Phys. 37 (2021) 2008033.
[33] A. Han, W. Chen, S. Zhang, et al., Adv. Mater. 30 (2018) e1706508.
[34] T. Zhang, X. Han, H. Yang, et al., Angew. Chem. Int. Ed. 59 (2020) 12055–12061.
[35] H. Zhou, Y. Zhao, J. Gan, et al., J. Am. Chem. Soc. 142 (2020) 12643–12650.
[36] B.W. Zhang, Y. Jiao, D.L. Chao, et al., Adv. Funct. Mater. 29 (2019) 1904206.
[37] K. Qi, X. Cui, L. Gu, et al., Nat. Commun. 10 (2019) 5231.
[38] J.C. Li, Y. Meng, L. Zhang, et al., Adv. Funct. Mater. 31 (2021) 2103360.
[39] W. Liu, W. Hu, L. Yang, J. Liu, Nano Energy 73 (2020) 104750.
[40] P. Sabhapathy, I. Shown, A. Sabbah, et al., Nano Energy 80 (2021) 105544.